tom. Physiol. Opt. 60, 278 (1983); National Institute for Occupational Safety and Health, *Criteria for a Recommended Standard, Occupational Exposure to Ultraviolet Radiation* (National Technical Information Service, Rockville, MD, 1972, Government Publication No. PB-214 268)]. Our subjects now wear UV-excluding clear Ultra-spec 2000 safety glasses (Uvex Winter Optical, Inc., Smithfield, RI) during bright light exposure, confirming that UV light is not responsible for the phase resetting observed.

39. Kronauer (*15*) suggests that the illuminance of light (as measured in lux) is related nonlinearly to its biological influence on the endogenous circadian pacemaker, and that the experimentally determined [S. S. Stevens, *Science* **133**, 80 (1961)] relation between illuminance (I) and perceived brightness (B), $B = CI^{1/3}$, might apply here. This has proved effective in the model simulation of laboratory bright light protocols [R. E. Kronauer and J. V. Frangioni, *Sleep Res.* **16**, 622 (1987)].

40. We thank the subject volunteers; the student research technicians; A. E. Ward, M. J. Matule, A. M. Sinz and M. P. Johnson for direct supervision of the studies; K. Whitmarsh and J. W. Jewett for subject recruitment; J. L. Anderson and S. A. Amira for psychological evaluations; S. Rogacz, J. Steinberg, and R. Mortensen for clinical evaluations; J. Swain, R. Salvador, and M. McCullough for the metabolic diets; L. Thorington for advice on designing the light banks; B. Potter and J. Norwood for hormonal assays; A. E. Ward, D. Sieburth and S. Lawson for the illustrations; M. Dumont, W. O. Freitag, J. Miner and S. H. Strogatz for suggestions on the manuscript; and G. H. Williams for his overall support of this work. Supported in part by grants NIA 1-RO1-AG06072, NIH DRR GCRC 5-M01-RR00888, NIH DRR BRSG 2-S07-RR-05950; by NIDDK training grant 5-T32-OK-07529 (E.N.B.); and by the Center for Design of Industrial Schedules. C.A.C. is a Sandoz Scholar in Medicine.

15 October 1988; accepted 4 May 1989

Water-Inserted α-Helical Segments Implicate Reverse Turns as Folding Intermediates

M. SUNDARALINGAM* AND Y. C. SEKHARUDU

Information relevant to the folding and unfolding of α helices has been extracted from an analysis of protein structures. The α helices in protein crystal structures have been found to be hydrated, either externally by a water molecule hydrogen bonding to the backbone carbonyl oxygen atom, or internally by inserting into the helix hydrogen bond and forming a hydrogen-bonded bridge between the backbone carbonyl oxygen and the amide nitrogen atoms. The water-inserted α-helical segments display a variety of reverse-turn conformations, such as type III, type II, type I, and opened out, that can be considered as folding intermediates that are trapped in the folding-unfolding process of α helices. Since the α helix, most turns, and the extended β strand occupy contiguous regions in the conformational space of φ, ψ dihedral angles, a plausible pathway can be proposed for the folding-unfolding process of α helices in aqueous solution.

ALL OF THE INFORMATION required for the tertiary folding of a protein is contained in its primary sequence (*1*). However, protein folding is a fast process that makes characterization of the folding intermediates difficult (*2, 3*). We have examined native protein structures for hints of what may have happened during their folding. We have found that a water molecule binds to an α helix, either externally to the backbone carbonyl O atom (Fig. 1A) or internally by prying open the helix hydrogen bond and lodging between the backbone carbonyl O atom and the amide group (Fig. 1B). The local conformations of the internally solvated α helices adopt an ensemble of classical reverse-turn conformations (*4*), types I, II, III, and open turns including the 3_{10} helix, that could represent trapped intermediates in the unfolding or folding of α helices. These intermediate structures occupy either common regions or are proximal to each other in the Ramachandran conformational space (*5*), and allow us to propose plausible folding pathways of α helices.

The impetus for this work began with our observations on the modes of hydration of α helices in troponin C (*6*), in which the exposed helix "handle" was surrounded by water molecules that hydrogen-bonded to the backbone carbonyl O atoms and the first turn of the B helix was disrupted by the insertion of water molecules into the helix hydrogen bonds. A similar binding of water molecules was simultaneously found in the structure of a small molecule, a synthetic oligopeptide analog containing α-aminoisobutyric acid residues (*7*). We surmised that these hydration schemes represent steps in the unfolding of α helices (*6*). The water-inserted segments displayed reverse-turn conformations, which suggested that the turn could be an incompletely folded helical segment that was trapped during the folding-unfolding of the α helices. Additional evidence for this arose when we noted the interchangeable occurrence of the helical segments and reverse turns in structures of the same protein from different sources: for example, phospholipase A2 residues 58 to 62, bovine (1BP2) (helical) versus porcine (1P2P) (turn); lysozyme 112 to 115, human (1LZ1) versus chicken (1LZT); acid protease residues 128 to 130, 161 to 163, and 176 to 178, penicillium (2APP) versus rhizopus (2APR). In the similarly folded chymotrypsin family of serine proteases, the helix content and the number of water-inserted segments differ, 2ALP (one helix), 3EST (two helices and one inserted segment, 233 to 237), 3RP2 (three helices and one inserted segment, 233 to 237), 2PTN (three helices and two inserted segments, 172 to 176 and 233 to 237), 4CHA (three helices and one inserted segment, 232 to 236), and 1TON (four helices and three inserted segments, 173 to 177, 232 to 236, and 233 to 237), again revealing the interchangeability of helical and nonhelical segments. In troponin C, there are four homologous calcium-binding helix-loop-helix motifs, namely, A, B; C, D; E, F; and G, H, but only the B helix contained inserted waters, whereas the other helices did not (*6*).

We collected hydrated α-helical segments from 35 protein structures (Table 1) that have been refined at a resolution of 1.9 Å or better from the Brookhaven Protein Data Bank (*8*). Only one structure from a family of proteins was included in our analysis. In serine proteases, one each from chymotrypsin and subtilisin families was used. We used the criterion that the hydrated "helical" segment should contain at least two residues in common with a helix, inclusive of the terminal residue, and also be compatible with retention of the adjacent helical conformation as visualized on a PS300 system using FRODO. Hence, we used $N - 3$ and $C + 3$ as helix boundaries, where N and C are the positions in the sequence of the helix terminal tersidues, as found in the Brookha-

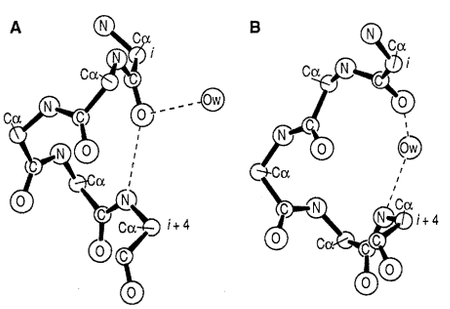

Fig. 1. The local pentapeptide segment of an α helix (**A**) with an externally bound water to the backbone carbonyl O atom, and (**B**) with an internally bound water bridging the backbone carbonyl O_i of the ith residue and the amide nitrogen atom N_{i+4}.

Department of Biochemistry, University of Wisconsin–Madison, Madison, WI 53706.

*To whom correspondence should be addressed.

ven Data Bank HELIX records. The search was performed over the length of the helices from $N - 3$ to $C + 3$ to extract the pentapeptide segments with externally bound waters, $CO_i \cdots NH_{i+4}$ and $CO_i \cdots Ow$ hydrogen bonds; the three-center transition state, $CO_i \cdots NH_{i+4}$, $CO_i \cdots Ow$, and $NH_{i+4} \cdots Ow$ hydrogen bonds; and internally bound waters, $CO_i \cdots Ow$ and $NH_{i+4} \cdots Ow$ hydrogen bonds. The hydrogen bonds were identified by the distances *d1*, *d2*, *d3*, *d2'*, and *d3'*, and the angles θ1, θ2, θ3, and θ4 (Fig. 2A) involving CO_i, N_{i+4}, H_{i+4}, and Ow atoms. The distances and angles involving the amide proton were obtained by fixing the proton at 1.0 Å from the amide N atom along the bisector of the angle C′N Cα. The water molecule was considered to hydrogen-bond to the helix carbonyl O atom when $d1 \leq 3.4$ Å and θ1 > 90°, and to the amide group when $d3 \leq 3.4$ Å and θ3 > 90°, in accordance with established criteria (*9*). Likewise, the helix hydrogen bond was considered to be present if $d2 \leq 3.4$ Å and θ2 > 90°. The average values of the angles were θ1 = 122° ± 9° and θ2 = 156° ± 12° in the external cases, θ1 = 127° ± 11°, θ2 = 155° ± 16°, and θ3 = 108° ± 13.0° in the three-centered cases, and θ1 = 135° ± 15° and θ3 = 152° ± 19° in the internal cases (the errors represent the standard deviations). In the three-centered cases where the amide proton is shared by both the carbonyl and the water O atoms, the absolute value of the pseudodihedral angle $H_{i+4} - N_{i+4} - Ow - O_i$ was 11° ± 8° and the sum of the angles θ2 + θ3 + θ4 around the amide proton was 325° ± 17°, implying the near planarity of the N_{i+4}, H_{i+4}, Ow, and CO_i atoms (*9*).

Table 1. The 19 proteins* that contain water-inserted and three-centered segments [see (*12*)].

Protein	Code†	Helix‡	Sequence§	Water‖	*d2*¶	*d3*
Azurin	2AZA	55–67	54–58 (A S Q I I)	167	5.5	3.0
		55–67	59–63 (V A T D G)	138	2.8	3.3
Bacteriochlorophyll-A protein	3BCL	183–190	184–188 (F A A I N/D)	60	4.3	3.1
		183–190	181–185 (G P A F A)	47	4.7	3.0
		284–297	291–295 (G M T G K)	114	4.4	2.9
		284–297	287–291 (L T H H G)	35	2.9	3.0
Carboxypeptidase A	5CPA	215–231	230–234 (L K S L Y)	444	4.6	2.8
		285–306	283–287 (A S Q I I)	491	4.8	3.0
Dihydrofolate reductase	3DFR	78–89	86–90 (A K N H L)	240	3.1	3.4
Hemoglobin	1ECD	117–133	116–120 (G A E A A)	88	5.9	3.0
		117–133	115–119 (A G A E A)	85	5.0	3.1
		76–88	75–79 (N I E A D)	55	5.9	3.4
Glutathione reductase	3GRS	444–453	441–445 (D E M L Q)	1	5.3	2.9
		299–304	296–300 (K D L S L)	158	6.1	3.0
		444–453	442–446 (E M L Q G)	24	5.7	3.1
		56–86	80–84 (D E M L Q)	248	5.4	2.9
		56–86	79–83 (M H D H A)	185	5.0	3.2
		444–453	451–455 (V K M G A)	408	4.3	3.3
Myoglobin (oxy)	1MBO	20–35	22–26 (A G H G Q)	122	3.0	3.1
		58–77	70–74 (T A L G A)	131	3.1	3.4
		58–77	62–66 (K K H G V)	122	3.2	3.4
		3–18	14–18 (W A K V G)	281	2.9	2.5
		3–18	15–19 (A K V E A)	281	3.7	3.4
Phospholipase A2	1BP2	89–108	94–98 (F I C N C)	37	3.1	3.4
Proteinase K	2PRK	244–256	246–250 (A S A C R)	96	5.9	3.2
		244–256	245–249 (A A S A C)	53	5.1	2.9
Ribonuclease A	1RN3	24–34	23–27 (S N Y C N)	250	5.2	3.0
Thermolysin	3TLN	260–274	258–262 (I G R D K)	528	4.9	3.2
		233–246	231–235 (H I N S G)	398	5.1	3.3
Tonin	1TON	231–244	233–237 (L K S L Y)	33	5.7	2.8
		231–244	232–236 (I K F T S)	91	5.2	3.4
		176–179	173–177 (K D N V T)	19	4.3	2.9
Lysozyme	2LZM	108–113	106–110 (M G E T G)	214	4.0	2.9
		93–106	103–107 (V F Q M G)	354	2.7	2.8
Cytochrome c peroxidase	2CYP	42–54	41–45 (G Y G P V)	345	5.4	3.1
Troponin c (chicken)	4TNC	41–48	39–43 (T K E L G)	240	4.9	3.1
		75–105	86–90 (M K E D A)	175	2.8	3.2
		75–105	88–92 (A D A K G)	183	3.2	3.4
		117–125	120–124 (E I L R A)	224	3.1	3.4
Citrate synthase	3CTS	373–386	375–379**	46	4.9	2.7
		373–386	376–380	47	5.9	3.1
		163–195	164–168	28	5.0	3.0
		221–236	221–226	83	3.3	3.2
		37–43	41–45	3	4.9	3.2
D-Glyceraldehyde-3-phosphate dehydrogenase	1GD1	210–215	209–213 (G A A K A)	467	2.7	3.3
		210–215	208–212 (T G A A K)	352	5.7	3.2
		10–18	7–11 (G F G R I)	356	6.0	3.4
Myohemerythrin	2MHR	71–84	74–78 (K K M H K)	184	3.0	3.4
		93–108	102–106 (W L V N H)	125	2.8	3.4
Cytochrome c2	3C2C	63–83	73–77 (N P K A F)	196	2.9	3.2

*The following 16 proteins do not contain the inserted segments: cytochrome c (3CYT), ferredoxin (4FD1), L7/L12 ribosomal protein (1CTF), ovomucoid third domain (1OVO), papain (9PAP), plastocyanin (5PCY), ubiquitin (1UBQ), acid proteinase (2APR), actinidin (2ACT), scorpion neurotoxin (1SN3), trp repressor (2WRP), cytochrome c3 (2CDV), insulin (1INS), trypsin inhibitor (5PTI), cytochrome c(prime) (2CCY), and ribonuclease T1 (1RNT). †Brookhaven Protein Data Bank (PDB) code. ‡Helix residues as in PDB. §Pentapeptide segment containing the water molecule. ‖As numbered in PDB. ¶In the three-centered cases, $d2 < 3.4$. **Amino acid sequence unknown.

The distances *d1*, *d2*, and *d3* were plotted in ascending magnitude of *d3* (Fig. 2B) to determine the influence of the approach of the water molecule to the amide group on the helix hydrogen bond. To the left of the transition state (Fig. 2B), there are a total of 50 cases. In 66% of these cases, the water molecule is inserted and hydrogen-bonded to both the carboxyl and the amide groups ($d3 < 3.4$ Å) and the helix hydrogen bond is broken ($d2 > 3.4$ Å) (Fig. 2B). In the remaining 34% of the cases, the helix hydrogen bond is not disrupted ($d2 < 3.4$ Å and $d3 < 3.4$ Å) and represents the three-centered cases. The structures with three-center hydrogen bonds can be regarded as intermediates in the transition between the externally and internally bound states. Of the 35 proteins, 15 contained water-inserted segments, 11 contained three-centered cases, and 27 contained externally bound segments. In all of these 35 proteins, there were 312 cases of hydrated segments, of which 262 were external, 17 were three-centered, and 33 were internal segments. Among the internally bound segments, 26 occur at the amino termini (CO_i located between $N - 3$ and $N + 3$), 4 at the carboxyl termini (CO_i located between $C - 3$ and C), and 3 within the helix (CO_i located between N + 3 and C − 3). Thus the water molecules can be inserted at any position along the helix, although they show a preference for the amino terminus. The insertion of a water molecule into the helix generally results in a kink or a directional change in the helix. The disposition of the external, three-center, and internal water molecules with respect to the carbonyl group of the peptide is shown in Fig. 2, C through E. The external and three-centered waters show a propensity for the outer lone-pair orbital and the internal wa-

ters for the inner lone-pair orbital.

Of the 262 segments, there were 63 cases with only CO_i externally bonded to a water molecule. The average values of the five pairs of the ϕ, ψ angles in these segments were: (i) −63°, −40°; (i + 1) −66°, −43°; (i + 2) −63°, −43°; (i + 3) −64°, −40°; and (i + 4) −65°, −41°. Nine segments showed distortions in the ϕ, ψ values that exceeded the average values by 3 SD and were omitted. The remaining 190 segments had one or more of the CO groups at i + 1, i + 2, i + 3 and i + 4 that were hydrogen-bonded to water molecules and thus were omitted in the calculation of the average ϕ, ψ values. The ϕ_{i+1}, ψ_i values are similar to those observed by Blundell *et al.* (*10*) for the α helices in hydrophilic environment (−66°, −41°) and deviate from the values found for the helices in hydrophobic environment (−59°, −44°) (*10*). The corresponding ϕ, ψ values of the three-centered cases, excluding four segments with deviations greater than 3 SD from the average ϕ, ψ, were: (i) −66°, −38°; (i + 1) −66°, −40°; (i + 2) −68°, −41°; (i + 3) −64°, −41°; and (i + 4) −61°, −36°. The perturbations in these values are small compared with those for buried helix; nevertheless, they display a tendency for distortion in the direction of a 3_{10} helix, −71°, −18°.

In the internally bound water segments, the conformational distortions are more diverse and the ϕ and ψ values (Fig. 3) are dispersed over the α helix, type-III turn, type-I turn, and occasionally in the type-II

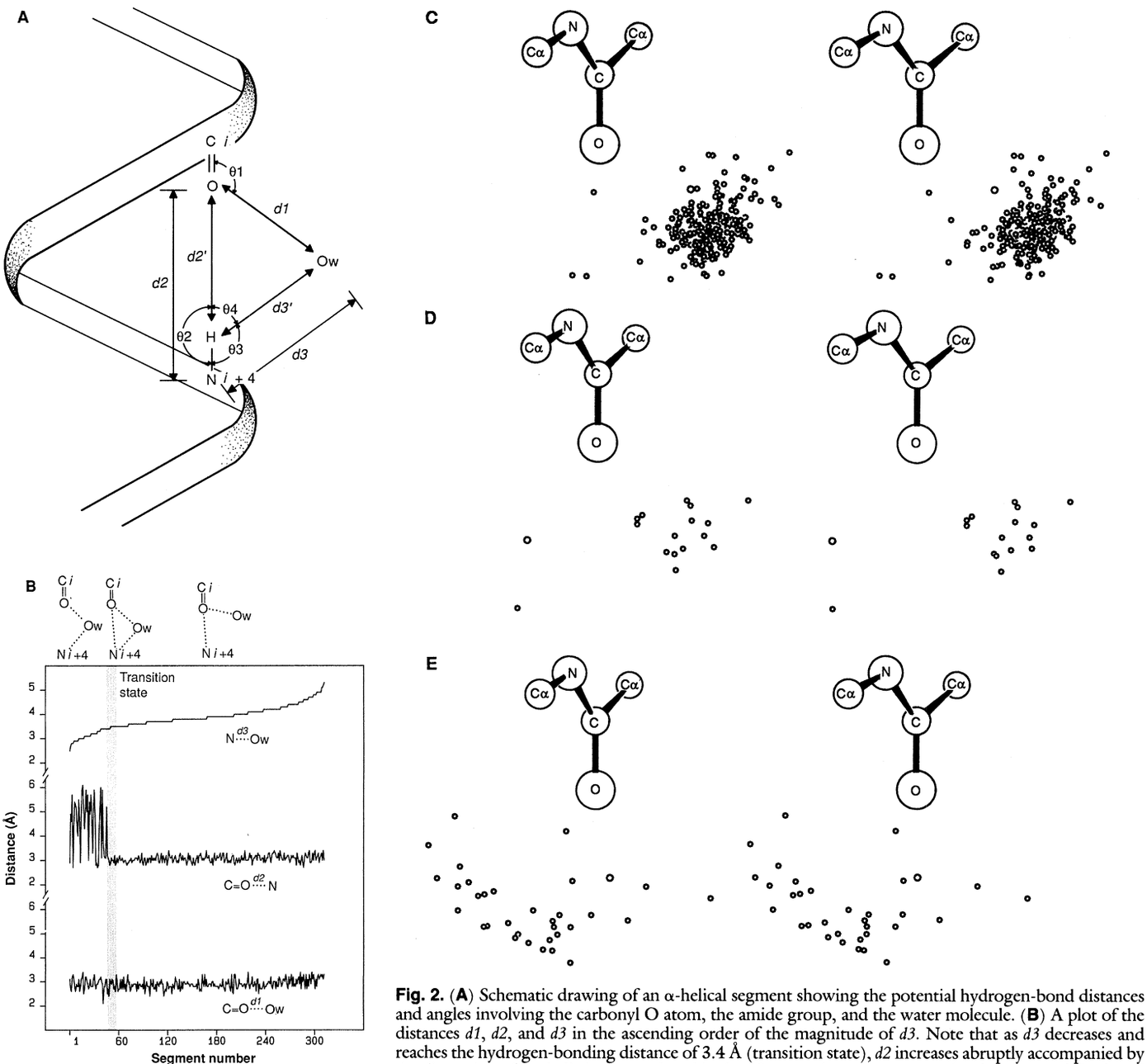

Fig. 2. (**A**) Schematic drawing of an α-helical segment showing the potential hydrogen-bond distances and angles involving the carbonyl O atom, the amide group, and the water molecule. (**B**) A plot of the distances *d1*, *d2*, and *d3* in the ascending order of the magnitude of *d3*. Note that as *d3* decreases and reaches the hydrogen-bonding distance of 3.4 Å (transition state), *d2* increases abruptly accompanied by the disruption of the helix hydrogen bond in the 33 cases where the water molecule is inserted. In the 17 three-centered cases, this dramatic change is not seen and the helix hydrogen bond is intact as in the external cases. (**C**) Stereoplot showing the distribution of the externally bound water molecules to the α helices in proteins. Note that the water molecules favor the direction of the outer lone-pair orbital of the O atom. (**D**) Stereoplot showing the distribution of the water molecules in the three-centered cases showing a preference for the outer lone-pair orbital as in (C). (**E**) Stereoplot showing the distribution of the water molecules in the internally bound segments which show a preference for the inner lone-pair orbital in contrast to (C) and (D).

turn and random coil or extended β regions. It appears that the water-inserted segments can adopt virtually the entire spectrum of the contiguous conformations in the ϕ, ψ space. The 21 segments with 4 → 1 hydrogen bonds represent the classical reverse turns, namely, types I, II, and III, and are centered at any of the four possible adjacent pairs of residues (i, $i + 1$; $i + 1$, $i + 2$; $i + 2$, $i + 3$; and $i + 3$, $i + 4$) in the pentapeptide segments. The type-III turns occur most frequently, followed by the type-I and type-II turns. The type-III and type-I reverse turns require only small perturbations in the ϕ, ψ values from an α helix. The type-II turns are restricted to the peptide segments with Pro-Gly sequences and require large conformational changes from an α helix. The remaining 12 segments that did not contain the 4 → 1 hydrogen bonds are open turns (*11*). These segments showed considerable conformational diversity that depended on the hydrogen-bonding geometry between the backbone carbonyl and amide groups and the bridging water molecule. In other words, the nature of the conformation adopted by the segments depended on the degree of "penetration" of the water molecule into the helical segment or on the "bite," that is, the distance of separation of the carbonyl and amide groups. The conformational states of the representative hydrated segments are shown in Fig. 4.

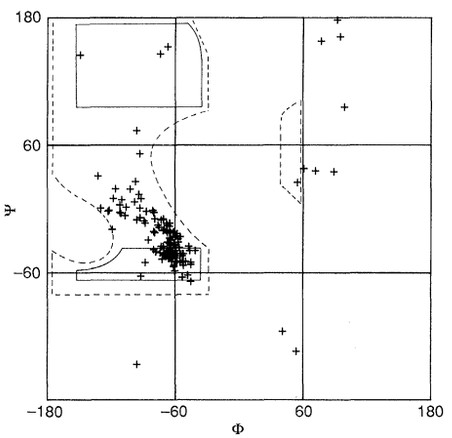

Fig. 3. The plot of the ϕ, ψ angles (indicated as crosses) of the water-inserted local pentapeptide segments, superimposed on a Ramachandran map. The distribution of the ϕ, ψ values indicates the considerable conformational flexibility displayed by these segments ranging from the various types of reverse turns to the open turn and the extended β strand. The water-inserted segments show a propensity for the "neck" region, comprising the type-I and type-III turns, indicating that the pathway in the conformational transition of the folding-unfolding process involves the turns. The crosses in the outlying regions are glycines.

The internal and external solvation of α helices is quite common in protein structures. The water-inserted segments, most interestingly, display virtually the entire range of conformations from the α helix to the extended β strand connected by the turns in the "neck" region of the ϕ, ψ space (Fig. 3). A comparison of the amino acid composition of the inserted segments (*12*) with that of reverse turns, α-helix termini, and α-helix middles (*13*) showed that the inserted segments are more similar to an α helix (termini or middle) (correlation coefficients, 0.81 and 0.78) than to reverse turns (correlation coefficient, 0.57). Thus these hydrated segments are potentially α helical and the series of conformations that they display could represent intermediates in the unfolding-folding process of α helices. Recent two-dimensional nuclear magnetic resonance studies (*14*) of a synthetic peptide (19 residues) having the sequence of the C helix of myohemerythrin in aqueous solution have indicated the presence of a set of turnlike structures in the carboxyl-terminal half, which were found to be rapidly interconverting between the folded and unfolded states. Our analysis identifies a role of water in the transition of the α helix to the random chain through various hydrated reverse turns and suggests that these reverse turns represent incompletely folded helical segments or trapped intermediates.

The gamut of water-mediated segments suggests ideas about the possible "conformational reaction coordinate" of the progressive unfolding of α helices in aqueous solution. The reaction coordinate may be represented by the structures that differ least in conformation, and therefore in energy, lying in the contiguous regions of the ϕ, ψ space that are both stereochemically and energetically permitted. It can be envisaged that α helices are initially solvated at the carbonyl O atoms (Fig. 4A) and three-center hydrogen bonds are formed (Fig. 4B). The water molecule could then pry open the helix hydrogen bond by inserting between the amide and carbonyl groups (Fig. 4, C through F). In this process the 5 → 1 hydrogen bond is broken and a 4 → 1 hydrogen bond is formed that leads to reverse turns. The type-III turn, by virtue of being closest to the α helix in conformational space, would be expected to be the initial intermediate encountered in the unfolding (Fig. 4C), followed by the type-I (Fig. 4D) or type-II (Fig. 4E) and the open turns (Fig. 4F). The reverse of this order would represent the folding process. The dynamics of unfolding may involve many water molecules, other interactions, and one or more of the above intermediates. However, the inserted water molecule seems to play a critical role in the folding or unfolding of the helix. Thus the conformational transition from the α helix to the extended chain or random coil perhaps traverses through various types of turns. Consequently, the family of hydrated reverse turns appears to play a central role in the formation of protein secondary structures. Thus the turns, besides being involved in the familiar chain reversal (*15*), also appear to be involved in the formation of the "linear" secondary structures driven by water molecules.

In the framework model of protein folding (*16*), the secondary structures are believed to be formed first and are then brought into proper interacting positions to form the tertiary structure through chain reversals involving loops and reverse turns, which are distinguished from the local re-

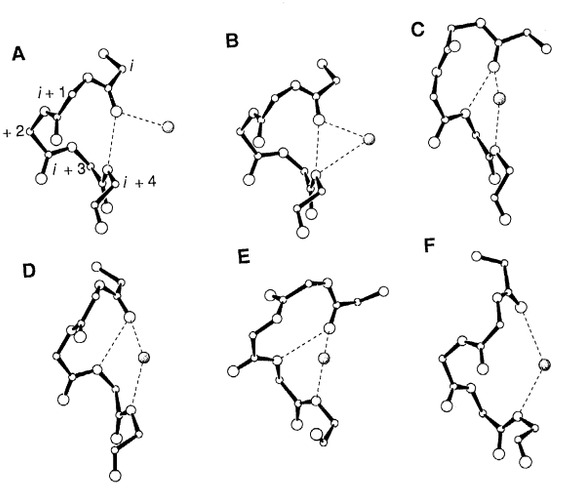

Fig. 4. Representative hydrated segments observed in protein crystal structures. (**A**) Water molecule bound externally only to helix carbonyl O atom (1ECD, residues 102 to 106, $d1$ = 2.8 Å, $d2$ = 2.9 Å, θ1 = 124°, and θ2 = 163°). (**B**) Water molecule bound to both the carbonyl and the amide groups, where the amide proton is involved in a three-center hydrogen bond (4TNC, residues 86 to 90, $d1$ = 2.7 Å, $d2$ = 2.8 Å, $d3$ = 3.2 Å, θ1 = 114°, θ2 = 170°, and θ3 = 116°; θ2 + θ3 + θ4 = 348°). (**C**) Insertion of a water molecule disrupting the helix hydrogen bond and the formation of a type-III turn (5CPA, residues 283 to 287, $d1$ = 3.1 Å, $d3$ = 3.0 Å, θ1 = 140°, and θ3 = 172°). (**D**) Same as (C), but forming a type-I turn (3GRS, residues 442 to 446, $d1$ = 2.9 Å, $d3$ = 3.1 Å, θ1 = 144°, and θ3 = 164°). (**E**) Same as (C) and (D), but forming a type-II turn (2PTN, residues 172 to 176, $d1$ = 2.8 Å, $d3$ = 3.0 Å, θ1 = 139°, and θ3 = 166°). (**F**) Insertion of a water molecule into the helix resulting in the disruption of the helix and turn hydrogen bonds and forming an open turn (2AZA, residues 54 to 58, $d1$ = 3.1 Å, $d3$ = 3.0 Å, θ1 = 143°, and θ3 = 153°). The above hydrated segments may be regarded as "snapshots" of the intermediates involved in the folding.

vese turns in the α helices discussed above. The reverse turns and loops in the proteins are generally exposed to the aqueous environment and are highly hydrated. Our preliminary analysis of the patterns of hydration of these loops and turns indicates that the water molecules again play an intimate role in directing the chain folding (*17*) and thus probably play a key role in driving protein folding.

REFERENCES AND NOTES

1. C. B. Anfinsen, *Science* **181**, 223 (1973).
2. P. E. Wright, H. J. Dyson, R. A. Lerner, *Biochemistry* **27**, 7167 (1988).
3. C. L. Tsou, *ibid.*, p. 1809.
4. C. M. Venkatachalam, *Biopolymers* **6**, 1425 (1968).
5. C. Ramakrishnan and G. N. Ramachandran, *Biophys. J.* **5**, 909 (1965).
6. K. A. Satyshur *et al.*, *J. Biol. Chem.* **263**, 1628 (1988), and unpublished results. The large difference in the interhelical angles of the apo calcium-binding motifs (AB 139° and CD 149°) probably stems from the B helix being kinked by the presence of inserted water molecules. In contrast, the interhelical angles of the holo calcium-binding motifs (EF 113° and GH 113°) are the same.
7. I. L. Karle, J. Flippen-Anderson, K. Uma, P. Balaram, *Proc. Natl. Acad. Sci. U.S.A.* **85**, 299 (1988).
8. F. C. Bernstein *et al.*, *J. Mol. Biol.* **112**, 535 (1977).
9. G. A. Jeffrey and J. Mitra, *J. Am. Chem. Soc.* **106**, 5546 (1984); G. A. Jeffrey, in *Landolt-Bornstein*, vol. VII/1, *Nucleic Acids*, W. Saenger, Ed. (Springer Verlag, Berlin, in press); U. C. Singh and P. A. Kollman, *J. Chem. Phys.* **83**, 4033 (1985).
10. T. L. Blundell, D. J. Barlow, N. Borkakoti, J. M. Thornton, *Nature* **306**, 281 (1983).
11. J. L. Crawford, W. N. Lipscomb, C. G. Schellman, *Proc. Natl. Acad. Sci. U.S.A.* **70**, 538 (1973).
12. The amino acid composition (in %) derived from the 26 inserted segments is: A, 16.15; G, 11.54; L, 5.38; I, 5.38; V, 3.08; F, 2.31; Y, 2.31; W, 0.77; P, 0.77; S, 6.92; T, 4.62; C, 2.31; M, 3.85; E, 6.92; D, 6.92; K, 8.46; R, 2.31; H, 3.85; O, 2.31; and N, 3.85. Abbreviations for the amino acid residues are: A, Ala; C, Cys; D, Asp; E, Glu; F, Phe; G, Gly; H, His; I, Ile; K, Lys; L, Leu; M, Met; N, Asn; P, Pro; Q, Gln; R, Arg; S, Ser; T, Thr; V, Val; W, Trp; and Y, Tyr. 3BCL with three inserted segments, which has only the x-ray sequence, and 3CTS with four inserted segments, whose sequence is unknown, were not included in calculation. Of the total of 130 residues in the 26 segments, Ala occurred 21 times and Gly 15 times. Composition of Ala and Gly in the inserted segments exceeded that of α helix middle by 3 and 6.5%, respectively.
13. The amino acid composition of the helix termini and the helix middle were extracted from P. Y. Chou and G. E. Fasman [*Adv. Enzymol.* **47**, 45 (1978)]. The helix termini include the three residues in either side of the helix boundaries and the α-helix middle excludes the three residues at the helix ends. The correlation coefficients given in the text were calculated using the relation $(Y_{est} = \overline{Y}_{est})^2/(Y = \overline{Y})^2$, where Y represents the amino composition of the inserted segments and Y_{est} represents the expected composition for the helix middles or reverse turns.
14. H. J. Dyson, M. Rance, R. A. Houghten, P. E. Wright, R. A. Lerner, *J. Mol. Biol.* **201**, 201 (1988). These authors (*ibid.*, p. 161) have also shown the presence of type-II and type-VI reverse turns in aqueous solution of a series of synthetic penta- and hexapeptide segments containing Pro and Gly by ^{1}H nuclear magnetic resonance studies. This result was expected for such sequences but was initially observed in solution by these workers. We find that water-inserted α-helical segments do not favor the type-VI reverse turn.
15. S. S. Zimmerman and H. A. Scheraga, *Proc. Natl. Acad. Sci. U.S.A.* **74**, 4126 (1977).
16. P. S. Kim and R. L. Baldwin, *Annu. Rev. Biochem.* **51**, 459 (1982).
17. M. Sundaralingam and Y. C. Sekharudu, unpublished results.

18. Supported by NIH grant AR-34139, the College of Agricultural and Life Sciences, and the University Graduate School. We dedicate this paper to G. A. Jeffrey, professor emeritus, Department of Crystallography, University of Pittsburgh.

7 December 1988; accepted 21 March 1989

Global Positioning System Measurements for Crustal Deformation: Precision and Accuracy

WILLIAM H. PRESCOTT, JAMES L. DAVIS, JERRY L. SVARC

Analysis of 27 repeated observations of Global Positioning System (GPS) position-difference vectors, up to 11 kilometers in length, indicates that the standard deviation of the measurements is 4 millimeters for the north component, 6 millimeters for the east component, and 10 to 20 millimeters for the vertical component. The uncertainty grows slowly with increasing vector length. At 225 kilometers, the standard deviation of the measurement is 6, 11, and 40 millimeters for the north, east, and up components, respectively. Measurements with GPS and Geodolite, an electromagnetic distance-measuring system, over distances of 10 to 40 kilometers agree within 0.2 part per million. Measurements with GPS and very long baseline interferometry of the 225-kilometer vector agree within 0.05 part per million.

RELATIVE MOTION OF THE MAJOR tectonic plates of the earth produces crustal deformation along the plate margins. This deformation typically involves strain rates of 0.1 to 0.5 ppm/year (*1*). Since late in the 19th century [for example, (*2*)], our understanding of crustal deformation has benefitted greatly from geodetic observations. Until recently, studies of the deformation occurring in plate boundary zones relied on data from triangulation, trilateration, and leveling. However, GPS surveying is rapidly becoming the preferred technique. In addition to providing a great deal of flexibility in selection of stations and a greater tolerance for adverse weather conditions and air quality than the older techniques, GPS provides a direct observation of three translation components and orientation. With land-based surveying, techniques must be combined in order to obtain all three translation components of station motion and the precision of the determination of the rotational part of the deformation is far below that of the other components. The ability to observe directly all translational components plus orientation between stations separated by any distance allows us to study plate deformation at broad scales over hundreds of kilometers as well as within a few meters in fault zones. Since late 1985, we have made repeated GPS measurements of the relative positions of stations in the western United States. In this report, we use this data set to examine the repeatibility of GPS vectors and to compare GPS measurements with those from other techniques.

The heart of GPS is a set of satellites (currently 7 active, but eventually 21) orbiting the earth at an altitude of approximately 20,000 km. These satellites transmit on two L-band frequencies, L_1 at 1575.42 MHz and L_2 at 1227.60 MHz. Receivers record time-tagged pseudo-range and phase observations (*3*) from L_1, L_2, or both. The signals broadcast by the satellites allow the user to determine the location of a single receiver with an accuracy of a few meters. For geodetic applications, at least two receivers are required. The satellite signals are then used in differential processing to determine the relative position of the receivers with an uncertainty 10^{-3} times as small as the measurement obtained with a single receiver.

The largest number of repeated observations are measurements of the relative positions of four stations in the vicinity of Parkfield, California (Fig. 1). Estimates of relative position were obtained from monthly GPS measurements (*4–10*), the series extending from January 1986 to October 1988. In all of the solutions, the coordinates of station 10JDG were fixed (*11*), and coordinates of the other three stations relative to station 10JDG were determined for each set of observations. The secular trends in station movement (Fig. 2) indicate that there was significant motion only in the component of velocity parallel to the strike of the San Andreas fault (Table 1). Rates obtained with GPS are consistent with other estimates of the creep rate (*12*) in the Parkfield area. The vertical component of one observation for station Joaquin is a clear outlier. We suspect that there was an error in the measurement of the antenna height.

The variations about the best fitting straight line are of particular interest for assessing the precision of the observations

U. S. Geological Survey, 345 Middlefield Road, Mail Stop 977, Menlo Park, CA 94025.